Check for updates

View Article Online
View Journal

ChemComm
Chemical Communications

Accepted Manuscript

This article can be cited before page numbers have been issued, to do this please use: M. Feßner, E. J. Tay, C. Grassin, S. Reese and C. Merten, *Chem. Commun.*, 2025, DOI: 10.1039/D5CC05078B.

This is an Accepted Manuscript, which has been through the Royal Society of Chemistry peer review process and has been accepted for publication.

Accepted Manuscripts are published online shortly after acceptance, before technical editing, formatting and proof reading. Using this free service, authors can make their results available to the community, in citable form, before we publish the edited article. We will replace this Accepted Manuscript with the edited and formatted Advance Article as soon as it is available.

You can find more information about Accepted Manuscripts in the Information for Authors.

Please note that technical editing may introduce minor changes to the text and/or graphics, which may alter content. The journal's standard Terms & Conditions and the Ethical guidelines still apply. In no event shall the Royal Society of Chemistry be held responsible for any errors or omissions in this Accepted Manuscript or any consequences arising from the use of any information it contains.

ROYAL SOCIETY OF CHEMISTRY

rsc.li/chemcomm

Please do not adjust margins

ChemComm

View Article Online
DOI: 10.1039/D5CC05078B

COMMUNICATION

Matrix-Isolation IR Spectra of Halogen-P and Halogen-π Complexes of Phosphines and Iodotrifluoroethylene (C_2F_3I)

Received 00th January 20xx,
Accepted 00th January 20xx

DOI: 10.1039/x0xx00000x

Malte Feßner, Elliot J. Tay, Corentin Grassin, Sven Reese, and Christian Merten*

Open Access Article. Published on 29 Septemba 2025. Downloaded on 01/10/2025 07:51:45.
This article is licensed under a Creative Commons Attribution 3.0 Unported Licence.

The C=C stretching mode of iodotrifluoroethylene (ITFE) serves as marker for halogen bonding (XB)-interactions in complexes with phosphines. The formation of a C-I···P XB-complexes becomes evident from a strong red-shift of this marker band. The formation of C-I···π bound clusters, which were kinetically trapped in the cryogenic environment, were confirmed by a slightly smaller red-shift of the marker band.

In its most general definition, a halogen bonding (XB) interaction[1-4] results from a net attraction between an electrophilic region of a halogen atom and a nucleophilic region in either the same or another molecule. In practice, halogen bonding donors are dihalogen compounds or haloorganics, and halogen bonding acceptors are entities that would also act as hydrogen bonding acceptors. The high directionality of XB-interactions finds applications in various fields, ranging from crystal engineering to catalysis[5, 6] and supramolecular chemistry.[7-10] Among the most utilized structural motifs are C-X bonds (with X = Br, I) interacting with nitrogen atoms of amines or the oxygens in carbonyl or ether groups. Halides,[11, 12] selenium,[13, 14] and sulfur[15] are also known to form halogen bonds.[16-20] Interestingly, although phosphines could also engage in XB-interactions, examples in literature are scarce. This lack of examples is due to the fact that the strongly polarizing phosphorous tends to abstract the halogen atom from the XB-donor,[21] resulting in formation of a covalent P-X bond. Most C-X···P halogen bonds reported in literature are thus reported in solid state and investigated by means of X-ray crystallography or solid-state NMR spectroscopy.[16, 22-24] Solely for the complex formed between triphenylphosphine and 1,3,5-trifluoro-2,4,6-triiodobenzene, not only solid state but also a solution-phase identification based on ^{31}P-NMR was reported.[22] An infrared (IR) spectroscopic characterization of such weakly bound C-X···P complexes in solution phase is hampered not only because of the potential reactivity of the mixture, but also because they may compete with solute-solvent interactions. Furthermore, band shifts associated with the complexes may be very small, so that the spectra would only slightly differ from those of the single components. Consequently, the broad bands of solution phase measurements simply prevent their identification. The technique of matrix isolation (MI) is well established for the characterization of conformational equilibria and intermolecular interactions as well as for studies on reactive intermediates. It involves the separation of target compounds and complexes in solid inert gas matrices, which are obtained by spraying mixtures of the components and an inert gas onto a spectroscopic window. The window is held at a temperature markedly below the melting point of the host gas (typically ~15–20 K), so that the arriving species are immediately frozen out. If the solid matrix is subsequently slightly warmed (annealing), small guest molecules can diffuse through the matrix and form clusters. As the rigid environment prevents any large amplitude structural rearrangements of larger guest molecules, the diffusion process may not only yield the thermodynamically most favourable complexes. In fact, high energy structures may become kinetically trapped.

Using matrix isolation and other cryogenic sampling techniques, the C=C stretching vibration of iodotrifluoroethylene (ITFE) has been identified as particularly sensitive probe for XB-interactions. As shown by Herrebout et al. in cryosolution experiments, *i.e.*, when using liquefied rare gases as solvents,[25, 26] XB-interactions of ITFE with amines lead to a strong shift of 10-15 cm^{-1}. For ferrocene and *N*,*N*-dimethyl ferrocenyl amine, we recently reported that ITFE also interacts with the π-faces of cyclopentadienyl giving C-I···π bound clusters under MI conditions.[27] Our detailed MI-IR study on ITFE itself revealed the presence of a particularly stable matrix site in argon, which

[a] Ruhr-Universität Bochum, Fakultät für Chemie und Biochemie, Organische Chemie II, Universitätsstraße 150, 44801 Bochum, Germany, E-mail: christian.merten@ruhr-uni-bochum.de, Web: www.mertenlab.de.

Supplementary Information available: experimental and computational details, additional experimental and computed spectra, energies, electrostatic potential maps, NCI analysis. See DOI: 10.1039/x0xx00000x

ChemComm Accepted Manuscript

persists when the matrix is annealed.[28] We subsequently identified para-hydrogen as an ideal environment to study complexes of ITFE, as no self-aggregation was observable under typical deposition conditions.[28] Notably, we also demonstrated that strong contributions of combination modes and overtones complicate the analysis of spectral regions around the other fundamental modes of ITFE.

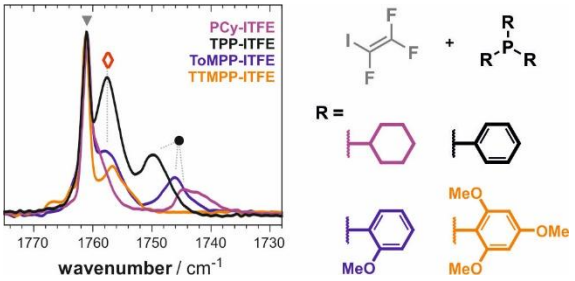

Figure 1. Experimental spectra of **ITFE** co-deposited with **PCy_3**, **TPP**, **ToMPP** and **TTMPP** in para-hydrogen matrix at 4 K in the range of the C=C stretching band of ITFE. The spectra are normalized to the band of monomeric ITFE (▼). Bands arising from complexes of the phosphines with ITFE are marked (●) and (◊). The full fingerprint range is presented in the ESI.

It was envisioned that ITFE could be the ideal probe to also characterize neutral XB-interactions with phosphines. For the present study, we thus recorded MI-IR spectra of **ITFE** co-deposited with tricyclohexyl phosphine (**PCy_3**), triphenyl phosphine (**TPP**), tris(o-methoxy phenyl)phosphine (**ToMPP**), and tris(2,4,6-trimethoxy phenyl)phosphine (**TTMPP**). In addition to the C=C stretching band of monomeric **ITFE**, which is observed at 1761.3 cm^{-1} (▼, Figure 1) in pH_2 matrix, the spectra of all four investigated systems showed additional bands in the C=C stretching regions indicative of complex formation during the deposition process. For three systems, a strongly red-shifted band (●) was observed (1744.6 cm^{-1} for **PCy_3**, 1746.1 cm^{-1} for **ToMPP**, 1749.8 cm^{-1} for **TPP**), which was apparently absent in the spectrum of **TTMPP**. Another sharp band (◊) was found at 1757.6 for **TPP** and **ToMPP**, and at 1756.7 cm^{-1} for **TTMPP**, respectively. In the same range, there is only a shoulder to the monomeric **ITFE** band visible near 1759 cm^{-1} for **ITFE-PCy_3**. In the remaining fingerprint region, new bands could also be observed near some of the other strong fundamental modes of ITFE (cf. Fig. S1). Most notably, very characteristic new bands occurred around the in-phase C-F stretching mode of **ITFE** ($\nu_{CF2,ip}$, 1004.5 cm^{-1}). In all four spectra, a new band at ~1002.3 cm^{-1} likely corresponds to the same species as the weakly shifted C=C stretching modes (◊). Further red-shifted bands occurred at 993.1 cm^{-1} for **ITFE-PCy_3** and 994.4 cm^{-1} for **ITFE-ToMPP**. There is likely also a band present ~997 cm^{-1} in the spectrum of **ITFE-TPP**, yet this range is overlapped with a band of **TPP** itself. For **TTMPP**, however, a similar band is clearly absent. The observed strongly shifted bands of $\nu_{CF2,ip}$ follow the same trend as the strongly shifted C=C stretching bands (●), suggesting that these bands belong to the same species. It is further noteworthy, that no changes for bands of the phosphines were observed as the XB-acceptors were deposited in large excess. Generally, the same trends can be observed in Ar-matrix after deposition (cf. Fig. S2) and annealing of Ar-matrices further intensified the complex bands.

View Article Online
DOI: 10.1039/D5CC05078B

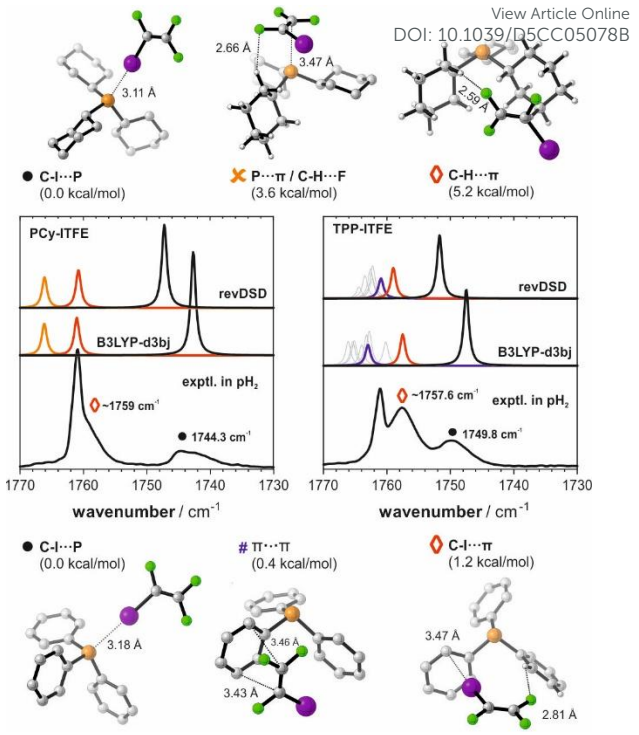

Figure 2. Comparison of computed IR spectra with the experimental spectra of **ITFE** and its complexes with **PCy_3** (left) and **TPP** (right) recorded in pH_2 matrix at 4 K. The analytically relevant section around the C=C stretching mode of **ITFE** is shown, as the remaining fingerprint region is of little diagnostic value. The figure also shows representative complex structures of **PCy_3-ITFE** (top) and **TPP-ITFE** (bottom), with bond lengths and relative ΔE_{ZPC} obtained at revDSD-PBEP86-d3bj/def2TZVP level. The grey spectra in the figure for **TPP-ITFE** correspond to other π···π structures.

For the computational analysis of **ITFE-PCy_3**, three types of intermolecular interactions were considered (Fig. 2). The C-I···P XB-interaction was found to be the most preferred at the utilized levels of theory, i.e., at B3LYP-d3bj[29] and revDSD-PBEP86-d3bj[30] level with def2TZVP basis. More than 3.5 kcal/mol less favourable is the second complex structure, which is best described as cooperative P···π /C-H···F interactions. Another 1.6-1.8 kcal/mol higher in energy is the third structure obtained for **ITFE-PCy_3**, which is stabilized by C-H···π interactions between a cyclohexyl ring and the ITFE molecule located above the ring. A structure with C-H···I interaction could not be obtained. Based on the computed harmonic IR spectra of these three structures, the strongly shifted band at 1744.6 cm^{-1} (●) could unambiguously be assigned to the C-I···P XB-complex ($\Delta\nu_{exp}$ = 16.7 cm^{-1}; $\Delta\nu_{B3LYP}$ = 18.6 cm^{-1}; $\Delta\nu_{revDSD}$ = 14.1 cm^{-1}). The calculations further suggested that the C-H···π interactions causes a very small red-shift of the C=C stretching band ($\Delta\nu_{exp}$ = ~2 cm^{-1}; $\Delta\nu_{B3LYP}$ = 0.3 cm^{-1}; $\Delta\nu_{revDSD}$ = 0.5 cm^{-1}), while the π-P/C-H···F interactions result in a blue-shift. Consistent also with the predicted shifts of the other fundamental modes of **ITFE** (cf. Fig. S3), the experimentally observed shoulder (◊) in the **PCy_3-ITFE** spectrum was thus assigned to a kinetically trapped C-H···π complex and it was concluded that the π··P/C-H···F complex is not formed under MI-conditions.

In the screening for complex structures of **TPP-ITFE**, we also found three general binding motifs. In addition to the C-I···P XB-

Open Access Article. Published on 29 Septemba 2025. Downloaded on 01/10/2025 07:51:45.
This article is licensed under a Creative Commons Attribution 3.0 Unported Licence.

ChemComm Accepted Manuscript

This journal is © The Royal Society of Chemistry 20xx

View Article Online
DOI: 10.1039/D5CC05078B

Open Access Article. Published on 29 Septemba 2025. Downloaded on 01/10/2025 07:51:45.
This article is licensed under a Creative Commons Attribution 3.0 Unported Licence.

structure, **ITFE** can interact with the π-faces of the aryl rings forming either C-I···π or π···π complexes (Fig. 2, bottom). The C-I··P complex was again found as the lowest energy structure, followed by several π···π structures (ΔE_{B3LYP} = 1.1-1.7 kcal/mol, ΔE_{revDSD} = 0.4-0.7 kcal/mol, cf. Tab. S1) and the C-I··π complex (ΔE_{B3LYP} = 2.0 kcal/mol, ΔE_{revDSD} = 1.2 kcal/mol). The computed vibrational spectra allowed for an unambiguous analysis of the experimental IR spectra of **TPP-ITFE**. The C=C stretching band in the C-I···P XB-complex again showed the largest shift (cf. Fig. 2), which nicely matched in magnitude with the experimentally observed values ($\Delta\nu_{exp}$ = 11.8 cm^{-1}; $\Delta\nu_{B3LYP}$ = 13.8 cm^{-1}; $\Delta\nu_{revDSD}$ = 9.6 cm^{-1}). Likewise, the strong band at 1749.8 cm^{-1} (◊) could directly be assigned to the C-I···π complex ($\Delta\nu_{exp}$ = 3.7 cm^{-1}; $\Delta\nu_{B3LYP}$ = 3.8 cm^{-1}; $\Delta\nu_{revDSD}$ = 2.3 cm^{-1}), as the π···π complexes are expected to be much closer to the ITFE monomer band. Again, the assignments were also consistent with the observed shifts in the spectral regions of the other fundamental modes of **ITFE** (cf. Fig. S4).

For the analysis of the **ToMPP-ITFE** and **TTMPP-ITFE**, we focused on spectra calculations at B3LYP-d3bj level of theory, as the increasing molecular size of the complexes made calculations at revDSD-PBEP86-d3bj not feasible anymore. In its lowest energy conformation, the three methoxy groups of **ToMPP** are oriented in the same direction, i.e., pointing towards the lone pair of the central phosphorous.[31] Under solution phase conditions, a coordination to the lone pair typically leads to the rotation of one aryl unit to decrease steric repulsion (see crystal structures of **ToMPP**-BH_3[32] or RhCl(**ToMPP**)(1,5-cyclo-octadiene)[33] for examples). Under matrix isolation conditions, however, such large amplitude motion required for this conformational change cannot take place. Hence, for the generation of **ToMPP-ITFE** structures, we assumed that the complex formation takes place solely with the lowest energy structure. Expectedly, the analysis of the IR spectrum of **ToMPP-ITFE** subsequently led to a very similar conclusion as for **TPP-ITFE** and it showed that C-I···P and C-I···π structures are present in the matrix (cf. Tab. S2 and Fig. S5).

Initially following the same approach as for **ToMPP**, we computed **TTMPP-ITFE** complexes based on the crystal structure conformation.[34, 35] Due to the steric crowding with two ortho-methoxy groups, **TTMPP** cannot adopt a symmetric propeller conformation with the three aryl rings being tilted in the same direction. Instead, one of the aryl rings arranges almost in plane with the lone pair of phosphorous. In a second low-energy structure of **TTMPP**, a methoxy group on the non-tilted aryl ring is rotated towards the phosphorous, which increases the steric shielding of the lone pair but lowers the zero-point corrected energy by about 0.2 kcal/mol (cf. Fig. 3 and S3). For both conformers of **TTMPP**, the C-I···P XB-complexes were found as most favourable complexes with **ITFE**. The shielding of the phosphorous with the methoxy group, however, introduced a drastic energy difference between the two C-I···P XB-complexes of 1.25 kcal/mol, clearly favouring the complex of the crystal structure-like conformer of **TTMPP** (cf. Fig. S6 for electrostatic potential maps). Notably, interactions with the methoxy oxygen atoms are significantly less favoured that with the phosphorous. Expectedly, the characteristic, strongly red-shifted band of the C=C stretching mode was predicted for both complexes yet it is absent in the experiment. The C=C stretching bands of **ITFE** in C-I···π structures coincided with those of C-I··O complexes, which could both well explain the band at 1756.7 cm^{-1} (◊). The π···π complexes could explain the small features seen at the high-energy side of the C=C stretching band of **ITFE**.

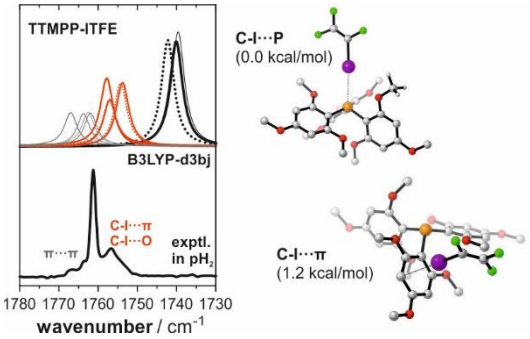

Figure 3. Comparison of the computed spectra of **ITFE-TTMPP** complexes with the experimental spectra recorded in para-hydrogen matrix at 4 K in the range of the C=C stretching band of **ITFE**. The dotted spectra correspond to structures of the second **TTMPP** conformation with the methoxy group rotated towards the phosphorous lone pair (cf. Tab S3). The grey spectra in the figure correspond to π···π structures.

From the computational analysis of the spectra, there is no apparent reason for the C-I···P XB-complexes being formed under matrix isolation only with **PCy_3**, **TPP** and **ToMPP**, but not with **TTMPP**. It confirmed the presence of higher energy complexes for all four phosphines, which are kinetically trapped and cannot rearrange towards the thermodynamically most preferred structures (*i.e.*, the C-I···P complexes). Notably, a comparison of the relative intensities of the diagnostic C=C stretching bands (● and ◊) suggested that the higher energy C-H···π and C-I···π states were the predominant species in the matrix. As the complex formation process under matrix isolation conditions is determined by diffusion processes within the deposited matrix, a mechanistic explanation for the lack of the C-I···P complex could be formulated. For the complex to form, **ITFE** must approach the phosphine in a suitable angle and ideally with the iodine first, and **ITFE** must have sufficient space around the phosphorous lone pair for it to move into a linear arrangement. With **TTMPP** being the sterically most demanding of the investigated phosphines based on the Tolman cone angles,[36] the chances for an encounter under these conditions is likely to be very limited. Instead, approaching **ITFE** molecules face the very attractive π-faces or slightly less preferable oxygen sites of the methoxy groups first and become kinetically trapped in higher energy π···π, C-I···π or C-I···O states (cf. Fig. S6 for electrostatic potentials). For **PCy_3**, **TPP** and **ToMPP**, the lone pairs are more exposed to the matrix environment and the approach is not shielded by methoxy groups. Consequently, as the lone pair represents also the most electronegative site for **PCy_3** and **TTP**, the statistical chance for the C-I···P XB-complex under MI conditions is notably increased.

The matrix isolation spectra presented in this study allow the key conclusion, that phosphines can engage in C-I···P halogen bonding interactions. They do not allow the converse

ChemComm Accepted Manuscript

View Article Online
DOI: 10.1039/D5CC05078B

conclusion, *i.e.*, that **TTMPP** cannot form XB-interaction through the phosphorous at all. Steric effects are likely to play a role in the complex formation process under matrix isolation conditions. Finally, it is interesting to note that there appears to be a certain correlation of the computed C-I···P bond distances in the ITFE-complexes of **PCy_3**, **TPP** and **ToMPP** with the frequency of the ITFE C=C stretching bands. Shorter distances lead to a stronger shift (cf. Tab. 1). However, when also considering the computed values for **TTMPP-ITFE**, it is not only the distance, but also secondary stabilizing interactions (cf. Fig. S7) that contribute to the shift of the C=C stretching band. Whether or not the position of the C=C stretching band has analytical value to compare XB-interactions among different complexes need to be explored in further detail in future studies.

Table 1. Comparison of the experimental band shift of the C=C stretching vibration ($\Delta\nu_{exp}$, cm^{-1}) with computed shifts ($\Delta\nu_{calc}$, cm^{-1}), C-I··P bond distances ($d_{C\text{-}I\cdot\cdot P}$, Å) and interaction energy ($\Delta E_{int} = E_{ZPC,complex} - E_{ZPC,phosphine} - E_{ZPC,ITFE}$; kcal/mol)

		B3LYP-d3bj			revDSD-PBEp86-d3bj	
	$\Delta\nu_{exp}$	$\Delta\nu_{calc}$	$d_{C\text{-}I\cdot\cdot P}$	ΔE_{int}	$\Delta\nu_{calc}$	$d_{C\text{-}I\cdot\cdot P}$
PCy3-ITFE	16.7	18.6	3.11	-11.0	14.1	3.16
ToMPP-ITFE	15.2	17.4	3.14	-12.2	--	--
TPP-ITFE	11.8	13.8	3.18	-8.4	9.6	3.24
TTMPP-ITFE	--	21.3	3.11	-15.6	--	--

We conclude this study by acknowledging financial by the Deutsche Forschungsgemeinschaft (DFG, German Research Foundation) under Germany's Excellence Strategy (EXC-2033, project no. 390677874), through the Research Training Group "Confinement Controlled Chemistry" (GRK 2376, project no. 331085229) and a research project (ME 4267/6-1, project no. 418662566). Further financial support was provided by the Mercator Research Center Ruhr (MERCUR, Pr-2017-0018).

Conflicts of interest

There are no conflicts to declare.

Data availability

The data supporting this article have been included as part of the Supplementary Information.

Notes and references

1. G. Cavallo, P. Metrangolo, R. Milani, T. Pilati, A. Priimagi, G. Resnati and G. Terraneo, *Chem. Rev.*, 2016, **116**, 2478-2601.
2. T. Clark, M. Hennemann, J. S. Murray and P. Politzer, *J. Mol. Model.*, 2007, **13**, 291-296.
3. M. Fourmigué, *Current Opinion in Solid State and Materials Science*, 2009, **13**, 36-45.
4. M. Erdelyi, *Chem. Soc. Rev.*, 2012, **41**, 3547-3557.
5. S. H. Jungbauer, S. M. Walter, S. Schindler, L. Rout, F. Kniep and S. M. Huber, *Chem. Commun.*, 2014, **50**, 6281-6284.
6. R. L. Sutar, E. Engelage, R. Stoll and S. M. Huber, *Angew. Chem. Int. Ed.*, 2020, **59**, 6806-6810.
7. P. Metrangolo, F. Meyer, T. Pilati, G. Resnati and G. Terraneo, *Angew. Chem. Int. Ed.*, 2008, **47**, 6114-6127.
8. L. C. Gilday, S. W. Robinson, T. A. Barendt, M. J. Langton, B. R. Mullaney and P. D. Beer, *Chem. Rev.*, 2015, **115**, 7118-7195.
9. A. Brown and P. D. Beer, *Chem. Commun.*, 2016, **52**, 8645-8658.
10. J. Y. C. Lim, I. Marques, V. Félix and P. D. Beer, *Angew. Chem. Int. Ed.*, 2018, **57**, 584-588.
11. S. Triguero, R. Llusar, V. Polo and M. Fourmigué, *Cryst. Growth Des.*, 2008, **8**, 2241-2247.
12. M. G. Chudzinski, C. A. McClary and M. S. Taylor, *J. Am. Chem. Soc.*, 2011, **133**, 10559-10567.
13. M. Iwaoka, T. Katsuda, H. Komatsu and S. Tomoda, *J. Org. Chem.*, 2005, **70**, 321-327.
14. H. D. Arman, E. R. Rafferty, C. A. Bayse and W. T. Pennington, *Cryst. Growth Des.*, 2012, **12**, 4315-4323.
15. D. Hauchecorne, A. Moiana, B. J. van der Veken and W. A. Herrebout, *Phys. Chem. Chem. Phys.*, 2011, **13**, 10204-10213.
16. K. Lisac, F. Topić, M. Arhangelskis, S. Cepić, P. A. Julien, C. W. Nickels, A. J. Morris, T. Friščić and D. Cinčić, *Nature Communications*, 2019, **10**, 61.
17. M. V. Chernysheva, J. M. Rautiainen, X. Ding and M. Haukka, *Journal of Solid State Chemistry*, 2021, **295**, 121930.
18. T. I. Madzhidov, G. A. Chmutova and Á. Martín Pendás, *J. Phys. Chem. A*, 2011, **115**, 10069-10077.
19. Y. Le Gal, A. Colas, F. Barrière, V. Dorcet, T. Roisnel and D. Lorcy, *CrystEngComm*, 2019, **21**, 1934-1939.
20. C. Laurence and J.-F. Gal, in *Lewis Basicity and Affinity Scales*, eds. C. Laurence and J.-F. Gal, John Wiley & Sons, Ltd2009, 10.1002/9780470681909.ch5, pp. 229-321.
21. V. Oliveira, E. Kraka and D. Cremer, *Phys. Chem. Chem. Phys.*, 2016, **18**, 33031-33046.
22. Y. Xu, J. Huang, B. Gabidullin and D. L. Bryce, *Chem. Commun.*, 2018, **54**, 11041-11043.
23. D. N. Zheng, P. M. J. Szell, S. Khiri, J. S. Ovens and D. L. Bryce, *Acta Crystallographica Section B*, 2022, **78**, 557-563.
24. A. M. Siegfried, H. D. Arman, K. Kobra, K. Liu, A. J. Peloquin, C. D. McMillen, T. Hanks and W. T. Pennington, *Cryst. Growth Des.*, 2020, **20**, 7460-7469.
25. D. Hauchecorne and W. A. Herrebout, *J. Phys. Chem. A*, 2013, **117**, 11548-11557.
26. Y. Geboes, F. De Proft and W. A. Herrebout, *J. Phys. Chem. A*, 2015, **119**, 5597-5606.
27. N. M. Kreienborg, F. Otte, C. Strohmann and C. Merten, *Phys. Chem. Chem. Phys.*, 2023, **25**, 15110-15114.
28. M. Feßner, J. Bloino and C. Merten, *Phys. Chem. Chem. Phys.*, 2025, **27**, 8377-8384.
29. S. Grimme, S. Ehrlich and L. Goerigk, *J. Comput. Chem.*, 2011, **32**, 1456-1465.
30. G. Santra, N. Sylvetsky and J. M. L. Martin, *J. Phys. Chem. A*, 2019, **123**, 5129-5143.
31. O. b. Shawkataly, M. A. A. Pankhi, I. A. Khan, C. S. Yeap and H.-K. Fun, *Acta Crystallographica Section E*, 2009, **65**, o1525-o1526.
32. N. P. Taylor, J. A. Gonzalez, G. S. Nichol, A. García-Domínguez, A. G. Leach and G. C. Lloyd-Jones, *J. Org. Chem.*, 2022, **87**, 721-729.
33. V. R. Landaeta, F. López-Linares, R. Sánchez-Delgado, C. Bianchini, F. Zanobini and M. Peruzzini, *Journal of Molecular Catalysis A: Chemical*, 2009, **301**, 1-10.
34. G. Nemeth, A. A. Pinkerton, J. A. Stowe and C. A. Ogle, *Acta Cryst. C*, 1992, **48**, 2200-2203.
35. K. R. Dunbar and S. C. Haefner, *Polyhedron*, 1994, **13**, 727-736.
36. J. A. Werra, K. Wurst, L. B. Wilm, P. Löwe, M. B. Röthel and F. Dielmann, *Organometallics*, 2023, **42**, 597-605.

Open Access Article. Published on 29 Septemba 2025. Downloaded on 01/10/2025 07:51:45.
This article is licensed under a Creative Commons Attribution 3.0 Unported Licence.

ChemComm Accepted Manuscript

The data supporting this article have been included as part of the Supplementary Information.

View Article Online
DOI: 10.1039/D5CC05078B

Open Access Article. Published on 29 Septemba 2025. Downloaded on 01/10/2025 07:51:45.
This article is licensed under a Creative Commons Attribution 3.0 Unported Licence.

ChemComm Accepted Manuscript